

Multi-Epoch High-Spectral-Resolution Observations of Neutral Sodium in 14 Type Ia Supernovae^{*}

A. Sternberg,^{1,2,†} A. Gal-Yam,³ J. D. Simon,⁴ F. Patat,⁵ W. Hillebrandt,¹ M. M. Phillips,⁶ R. J. Foley,⁷ I. Thompson,⁶ N. Morrell,⁶ L. Chomiuk,⁸ A. M. Soderberg,⁹ D. Yong,¹⁰ A. L. Kraus,¹² G. J. Herczeg,¹³ E. Y. Hsiao,⁶ S. Raskutti,¹⁴ J. G. Cohen,¹⁵ P. A. Mazzali,^{1,16} and K. Nomoto,¹⁷

¹ Max Planck Institute for Astrophysics, Karl Schwarzschild St. 1, 85741 Garching bei München, Germany

² Minerva Fellow

³ Benoziyo Center for Astrophysics, Faculty of Physics, Weizmann Institute of Science, Rehovot 76100, Israel

⁴ Observatories of the Carnegie Institution for Science, 813 Santa Barbara St., Pasadena, CA 91101, USA

⁵ European Southern Observatory, Karl Schwarzschild St. 2, 85748 Garching bei München, Germany

⁶ Carnegie Observatories, Las Campanas Observatory, Casilla 601, La Serena, Chile

⁷ Department of Astronomy, University of Illinois Champagne-Urbana, MC-221, 1002 W. Green Street, Urbana, IL 61801, USA

⁸ Department of Physics and Astronomy, Michigan State University, East Lansing, MI 48824, USA

⁹ Harvard-Smithsonian Center for Astrophysics, 60 Garden Street, Cambridge, MA 02138, USA

¹⁰ Research School of Astronomy and Astrophysics, Australian National University, Canberra, ACT 2611 Australia

¹¹ Institute of Astronomy, University of Hawaii, 2680 Woodlawn Drive, Honolulu, HI 96822, USA

¹² Department of Astronomy, The University of Texas at Austin, 2515 Speedway, Stop C1400, Austin, Texas 78712-1205, USA

¹³ Kavli Institute for Astronomy and Astrophysics, Peking University; Yi He Yuan Lu 5, Hai Dian Qu, Beijing 100871, China

¹⁴ Department of Astrophysics, Princeton University, Princeton, NJ 08540, USA

¹⁵ Department of Astrophysics, California Institute of Technology, MC 249-17, Pasadena, CA 91125, USA

¹⁶ Astrophysics Research Institute, Liverpool John Moores University, Liverpool L3 5RF, United Kingdom

¹⁷ Kavli Institute for the Physics and Mathematics of the Universe (WPI), The University of Tokyo, Kashiwa, Chiba 277-8583, Japan

Released 2013xxxx XX

ABSTRACT

One of the main questions concerning Type Ia supernovae is the nature of the binary companion of the exploding white dwarf. A major discriminant between different suggested models is the presence and physical properties of circumstellar material at the time of explosion. If present, this material will be ionized by the ultra-violet radiation of the explosion and later recombine. This ionization-recombination should manifest itself as time-variable absorption features that can be detected via multi-epoch high-spectral-resolution observations. Previous studies have shown that the strongest effect is seen in the neutral sodium D lines. We report on observations of neutral sodium absorption features observed in multi-epoch high-resolution spectra of 14 Type Ia supernova events. This is the first multi-epoch high-resolution study to include multiple SNe. No variability in line strength that can be associated with circumstellar material is detected. We find that $\sim 18\%$ of the events in the extended sample exhibit time-variable sodium features associated with circumstellar material. We explore the implication of this study on our understanding of the progenitor systems of Type Ia supernovae via the current Type Ia supernova multi-epoch high-spectral-resolution sample.

Key words: Supernovae: general – circumstellar matter – ISM: general.

1 INTRODUCTION

Type Ia supernovae (SNe Ia) are widely accepted to be the thermonuclear explosion of accreting carbon-oxygen white-dwarfs (WDs) in close binary systems (Hoyle & Fowler 1960). Despite numerous studies the nature of the companion of the exploding WD still remains uncertain. Presently, there are two models that are widely accepted as plausible descriptions of SN Ia progenitor

^{*} Partially based on observations made with ESO Telescopes at the La Silla Paranal Observatory, Chile, under programme ID 289.D-5023, 290.D-5010, 290.D-5023, 091.D-0780.

[†] E-mail: asternberg@mpa-garching.mpg.de

systems. In the first model, the single-degenerate (SD) model, the companion is a non-degenerate star that transfers mass onto the WD (Whelan & Iben 1973). In a second, the double-degenerate (DD) model, the secondary is a WD (Iben & Tutukov 1984; Webbink 1984). A third model, less widely accepted at present, is the core-degenerate (CD) model in which a WD merges with the core of an evolved star during, or shortly after, the common-envelope phase (Sparks & Stecher 1974; Livio & Riess 2003; Kashi & Soker 2011; Ilkov & Soker 2012). One of the major differences between current alternative models is the properties of the gaseous environment surrounding the WD at the time of explosion. Therefore, detection of absorption by circumstellar material (CSM) in the spectra of SNe Ia, or the lack thereof, and the study of its properties might help to disentangle the plausible from the implausible progenitor systems.

Patat et al. (2007b, hereafter P07) were the first to report the detection of circumstellar material in a SN Ia, SN 2006X, based on time-variability observed in the neutral sodium (Na I) D absorption lines (restframe wavelengths $\lambda\lambda 5890, 5896$). The lack of time variability in the Ca II H & K lines led P07 to conclude that the observed change in the sodium absorption features was due to the ionization and recombination of circumstellar material, and not a geometrical line-of-sight effect. P07 based their conclusion arguing that SN Ia UV radiation is severely line-blocked by heavy elements bluewards of 3500\AA (Pauldrach et al. 1996; Mazzali 2000), and is therefore capable of ionizing only material that is relatively near the explosion. If the material density is sufficiently high it will recombine after maximum light giving rise to variability in observed absorption features. They suggested a single-degenerate progenitor system for SN 2006X. Following P07 similar studies provided a mixture of results both of detection of time-variable absorption features associated with CSM - SN 2007le (Simon et al. 2009), SN 1999cl (Blondin et al. 2009, using low-spectral-resolution) and PTF 11kx (Dilday et al. 2012) - and of non-detection of such features - SN 2000cx (Patat et al. 2007a), SN 2007af (Simon et al. 2007). Patat et al. (2013) detected marginally significant time-variability in the sodium features of SN 2011fe that were anyway compatible with interstellar material (ISM) and not with CSM. This mixture of results suggests that SNe Ia might actually arise from two types of progenitor systems, as is suggested by other studies (Mannucci, Della Valle & Panagia 2006; Sullivan et al. 2010; Wang et al. 2013; Maguire et al. 2013). The published sample of SNe with multiple high-resolution spectra is too small to allow for a significant conclusion to be drawn. Moreover, it also prevents us from deriving a robust ratio between SNe Ia that show evidence of CSM and those that do not. For that, a larger sample of SN Ia multi-epoch high-resolution spectra is needed.

Sternberg et al. (2011, hereafter S11) adopted a different approach based on a statistical analysis of a single-epoch high-spectral-resolution sample consisting of 35 SN Ia events. S11 showed that SNe Ia in nearby spiral hosts exhibit a statistically significant overabundance of features that are blueshifted relative to the strongest absorption feature, and this was interpreted as evidence of outflows from $\sim 20 - 25\%$ of their progenitor systems. Foley et al. (2012) showed that events classified as blueshifted \dot{a} Ia S11 tend to have higher ejecta velocities and redder colors at maximum light compared to the rest of the SN Ia sample. Maguire et al. (2013) used a classification scheme slightly different than that used by S11 to analyze an extended sample consisting of the S11 sample and an additional 17 intermediate-resolution single-epoch spectra, showing a $\sim 20\%$ excess of events with blueshifted features. These analyses lend strong support to the existence of CSM in a

non-negligible fraction of SNe Ia and the possibility of a bimodal distribution of SN Ia progenitors. Nevertheless, one cannot use the S11 sample or the Maguire et al. sample to study the properties of the CSM as it is not possible to confidently distinguish between CSM and ISM features for an individual SN in single-epoch spectra. Multi-epoch observations are needed.

In this paper we present multi-epoch high-spectral-resolution observations of 14 Type Ia events, some of which are from the S11 sample for which only single-epoch spectra were previously published. Publication of such data will help make the published SN Ia multi-epoch high-spectral-resolution sample more complete. We use this data set, plus literature observations of six other SNe, to provide the first robust estimate of the fraction of SNe Ia exhibiting variable absorption. We discuss the robustness of the time-variability non-detection and how this effects the consistency of the current multi-epoch high-spectral-resolution sample with previous studies.

2 DATA

Observations were performed using either the Ultraviolet and Visual Echelle Spectrograph (UVES; Dekker et al. 2000) mounted on the Very Large Telescope array (VLT) UT2, the High Resolution Echelle Spectrograph (HIRES; Vogt et al. 1994) mounted on the Keck I telescope, the Magellan Inamori Kyocera Echelle (MIKE; Bernstein et al. 2003) spectrograph mounted on the Magellan II Clay telescope, and the East Arm Echelle (EAE; Libbrecht & Peri 1995) spectrograph mounted on the 200 inch Hale telescope at Palomar. Information regarding the discovery and spectroscopic observations of individual SNe can be found in appendix A. UVES data were reduced using the latest ESO Reflex reduction pipeline. HIRES spectra were reduced using the MAuna Kea Echelle Extraction (MAKEE) data reduction package (written by T. Barlow; <http://spider.ipac.caltech.edu/staff/tab/makee/>). MIKE spectra were reduced using the latest version of the MIKE pipeline (written by D. Kelson; <http://code.obs.carnegiescience.edu/mike/>). EAE data were reduced using standard IRAF routines.

3 RESULTS

Using the IRAF RVCORRECT and DOPCOR routines we applied the appropriate heliocentric correction to all the spectra. Using the IRAF SPLLOT routine we normalized the spectra, measured the RMS and the signal to noise ratio (S/N) on the continuum in the vicinity of the D₂ and D₁ lines. We removed telluric features using a synthetic telluric spectrum produced by the Line By Line Radiative Transfer Model (Clough et al. 2005) based on the HITRAN database (Rothman et al. 2009). For more details see Patat et al. (2013, their Appendix A). We measured the equivalent width (EW) of the absorption features using the RMS as the σ_0 parameter in the SPLLOT error estimation. EW errors ignore continuum placement. Values of EW, error, S/N, and the D₁ to D₂ ratio for each epoch are given in Table 1. Comparisons between the first epoch and every subsequent epoch obtained for each SN are presented in Figs. 1-14. First epoch spectra are in blue and subsequent epochs in red. The black line in the narrow panel of each figure is the difference spectrum, i.e., the subtraction of the earlier epoch spectrum from the later one. For comparison we present the EW, error and S/N measurements for SN 2006X, SN 2007le and PTF 11kx in Table 2. We performed the measurements for

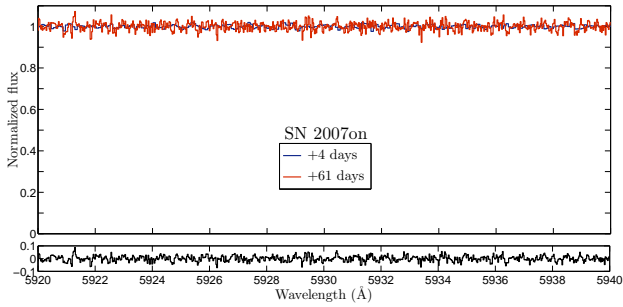


Figure 1. The dual-epoch spectra of SN 2007on. The first epoch is given in blue while the second is given in red. The difference spectrum (black line; in units of normalized flux) is given in the narrow panel at the bottom of the plot. Based on the host galaxy redshift, $z = 0.006494$, the host/SN Na I D features are expected to appear around 5928\AA & 5934\AA (for the D_2 and D_1 , respectively). No features are observed.

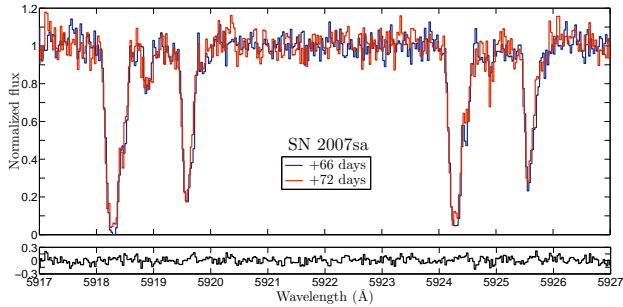


Figure 2. The dual-epoch spectra of SN 2007sa. The first epoch is given in blue while the second is given in red. The difference spectrum (black line) is given in the narrow panel at the bottom of the plot.

SN 2006X and PTF 11kx and used the measurements previously published for SN 2007le (Simon et al. 2009). Fig 15 shows a plot of the EW change as a function of days since maximum light for these three cases, SN 2007on, SN 2007C, and SN 2011iy.

In Fig. 1 we present a comparison between the two spectra of SN 2007on. Based on the host galaxy redshift, $z = 0.006494$ (Graham et al. 1998), the SN or host sodium features should have been visible, if present, within the given range. Both epochs seem to be featureless and are to show that there is no significant difference between them. The difference spectrum does not reveal any significant change between the two epochs. The EW values of the D_2 and D_1 lines are consistent with zero.

In Fig. 2 we present the region of the Na I D features observed in SN 2007sa spectra that are consistent with the SN or host galaxy redshift. Both epochs are overplotted to show that there is no significant difference between them. Moreover, the difference spectrum does not reveal any significant change that is not within the noise level. Though the EW values of the D_2 and D_1 lines show a slight decreasing trend between the first and the second epoch they are still consistent within the calculated errors, 1.2σ and 2.7σ for the D_2 and D_1 lines respectively. Given the small time separation between the two epochs and the lateness of the first spectrum, we consider it unlikely that these changes are real.

In Fig. 3 we present the sodium region of the multi-epoch spectra of SN 2007sr. These five epochs were obtained using three different spectrographs - MIKE, EAE, and HIRES. Though some apparent variability can be seen the D_2 EW values measured for all

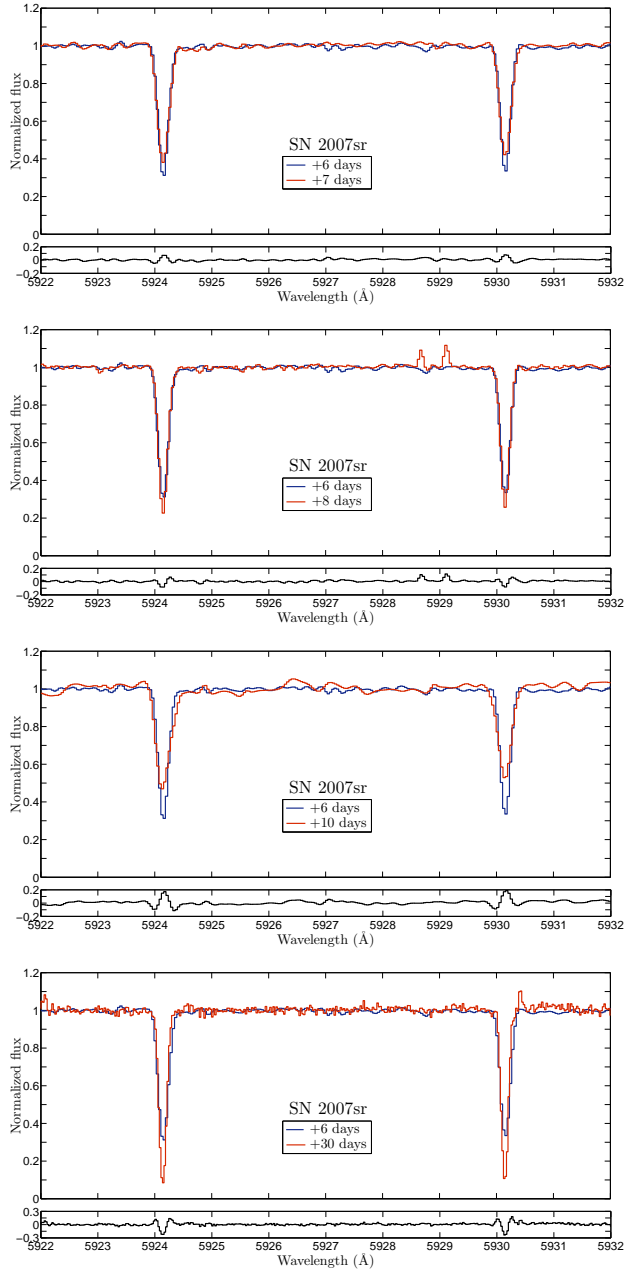


Figure 3. The multi-epoch spectra of SN 2007sr. Each plot shows a comparison of the first epoch (blue) and one of the other four epochs (red). The black lines given in the lower panel of each plot is the difference spectrum. As the measured EW of the different epochs are consistent with one another the observed difference in the line profiles are due to the different resolution of the spectrographs used on the different epochs.

epochs are all consistent within the calculated errors. The changes in the D_1 measurements in the fourth and fifth epochs are close to the 4σ level but are most likely not real, rather due to normalization of the spectrum near the edge of the D_1 line, and they do not appear in the stronger D_2 lines. The observed variability can be attributed to the difference between the spectral resolution of the three instruments.

An examination of the SN 2008C spectra in Fig. 4 does not reveal lines that are significantly variable in both lines of the sodium doublet. Though the EW values exhibit a slight decreasing trend

Table 1. Measurements for the observed events.

	Phase ¹	Instrument	EW (mÅ)		D ₁ /D ₂ ²	S/N
			D ₂	D ₁		
SN 2007on	+4	MIKE	4±6	0±5	N/A	116
	+61	HIRES	0±8	0±6	N/A	48
SN 2007sa	+66	HIRES	558±11	475±11	0.85	21
	+72	HIRES	538±13	429±13	0.8	18
SN 2007sr	+6	MIKE	152±2	146±2	0.96	109
	+7	MIKE	152±2	137±2	0.9	112
	+8	MIKE	152±2	138±2	0.91	117
	+10	EAE	152±4	120±4	0.79	51
	+30	HIRES	153±2	126±2	0.82	104
SN 2008C	+16	HIRES	637±10	444±10	0.7	34
	+22	HIRES	624±15	423±16	0.68	22
SN 2008dt	+6	HIRES	409±33	287±33	0.7	10
	+12	HIRES	490±32	325±32	0.66	11
	+18	HIRES	430±25	354±25	0.82	13
SN 2009ds	+7	MIKE	676±5	497±5	0.74	74
	+24	MIKE	704±6	510±6	0.72	68
SN 2010A	-8	MIKE	453±3	308±4	0.68	90
	-7	MIKE	456±3	284±4	0.62	88
	+14	MIKE	448±7	301±9	0.67	37
SN 2011iy	+64	MIKE	1314±5	1066±5	0.81	69
	+166	MIKE	1286±26	1077±25	0.84	13
SN 2012cu	+8	MIKE	928±6	857±6	0.92	79
	+24	MIKE	936±7	851±7	0.91	61
	+36	UVES	918±6	838±6	0.91	33
	+49	UVES	919±8	851±8	0.93	24
SN 2012fr	-5	UVES	0±2	0±2	N/A	111
	+7	UVES	0±2	0±2	N/A	119
	+18	UVES	0±4	3±4	N/A	83
	+39	UVES	9±3	28±3	N/A	102
	+96	MIKE	10±11	18±11	N/A	52
SN 2012hr	+7	MIKE	133±3	102±4	0.77	123
	+37	MIKE	122±8	120±9	0.98	45
SN 2012ht	-2	MIKE	0±4	1±4	N/A	148
	+5	UVES	3±4	5±4	N/A	67
	+7	MIKE	0±9	0±9	N/A	66
	+12	UVES	4±7	5±7	N/A	33
	+24	UVES	1±3	0±3	N/A	70
SN 2013aa	-1	MIKE	0±3	0±3	N/A	182
	+7	UVES	2±3	0±3	N/A	96
	+12	UVES	1±2	0±2	N/A	101
	+22	UVES	2±3	1±3	N/A	69
	+56	UVES	4±5	2±5	N/A	46
SN 2013aj	+3	UVES	89±2	57±2	0.64	73
	+35	UVES	83±6	51±6	0.62	28

¹ In days since max.² For events that do not exhibit sodium lines the ratio is marked as N/A.

they are consistent with one another as they are in agreement within $\sim 1\sigma$. In addition, the decrease in EW is counter to the expected behavior from ionization-recombination. Rather, this decrease, if it were significant, would be consistent with ongoing ionization at epochs that are a 16 and 22 days after maximum light.

Each panel of Fig. 5 shows comparisons between second (up-

per) or third (lower) epoch and the first epoch of SN 2008dt. Though some lines exhibit a visible change, these changes are all within the variations expected due to noise. This can be seen quite clearly in the difference spectra. Moreover, when we examine the EW values we see that the D₂ and the D₁ line seem to show different trends. As the sodium D lines are a doublet, a real trend should

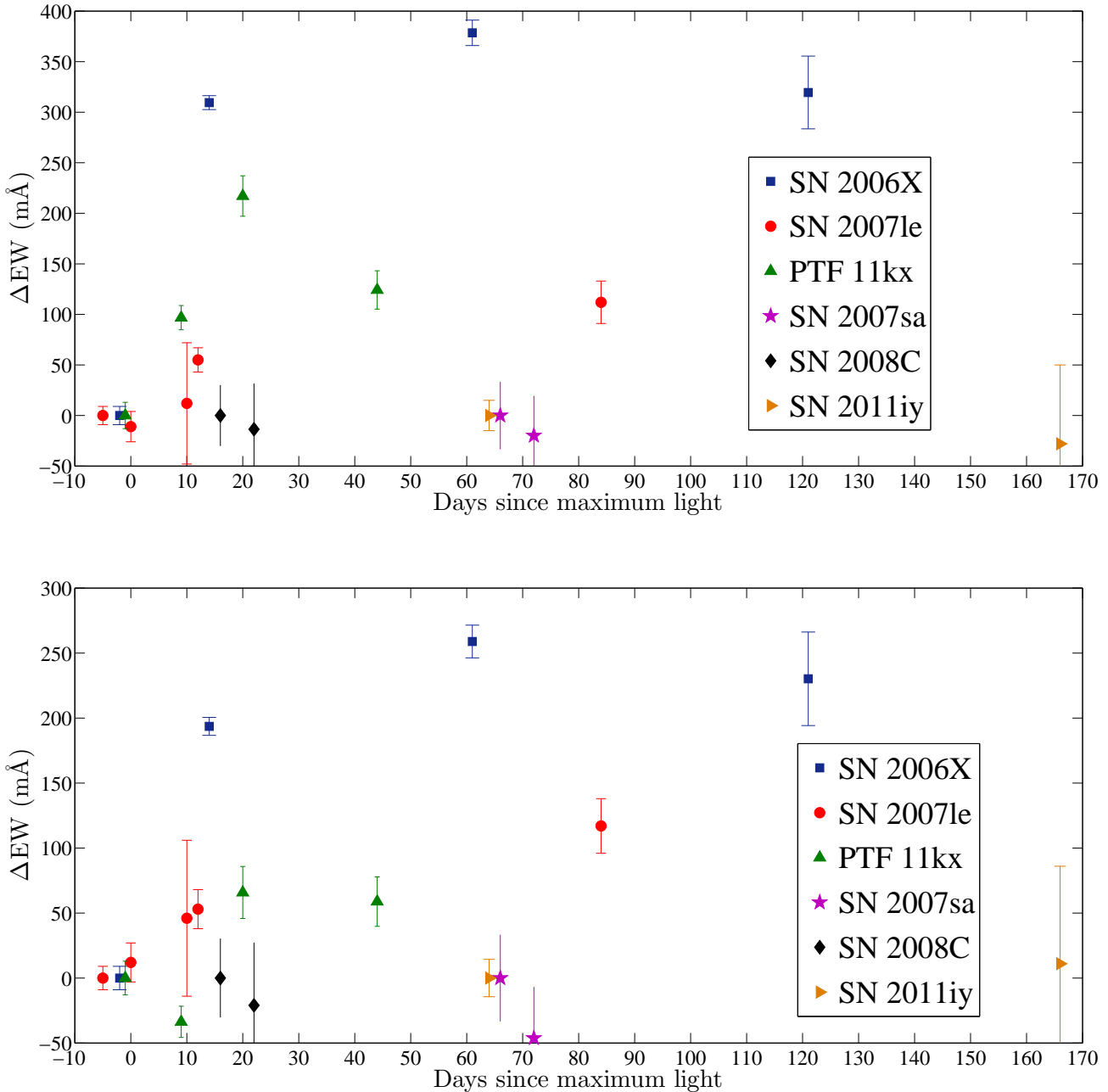


Figure 15. Changes in the EW of previously published events SN 2006X, SN 2007le, and PTF 11kx as a function of days since maximum light. The upper panel presents the change in the D₂ line and the lower in the D₁ lines. The error bars represent 3 σ errors. The data points for SN 2007sa, SN 2008C, and SN 2011iy are plotted to show that their observations were either performed on epochs too closely spaced apart or that their first epochs were obtained too late.

manifest itself in the same manner in both lines. Moreover, given the error estimates the EW values of the three epochs are consistent with one another well within the 2 σ level.

The dual-epochs of SN 2009ds are presented in Fig. 6. The difference spectra given in the lower panel demonstrate that the slight changes between the two epochs are well within the noise level. EW values of the D₁ lines are consistent with one another. The EW values of the D₂ show a larger difference and an agreement of only 3.6 σ . If we look at the EW of the D₁ and D₂ lines combined we see that the two epoch show a difference of 3.7 σ . This is a small but significant detection of time variability. Whether or not

this variability can be associated with CSM will be discussed in §4. The two epochs are spread over a period that spans the previously detected time-variability phase.

Examination of Fig. 7 does not reveal significant variations in the absorption line profiles observed in the spectra of SN 2010A. All variations in the D₂ lines are in agreement with the S/N and the calculated errors, at the 1 σ level or below. However, the EW of the D₁ lines of the second epoch does not agree with the first epoch at a 4 σ level. Nevertheless, the EW of the D₁ lines in the second and third epoch agree on a 1.7 σ level and between the first and third epoch on a 0.7 σ level. Moreover, if this variability were true,

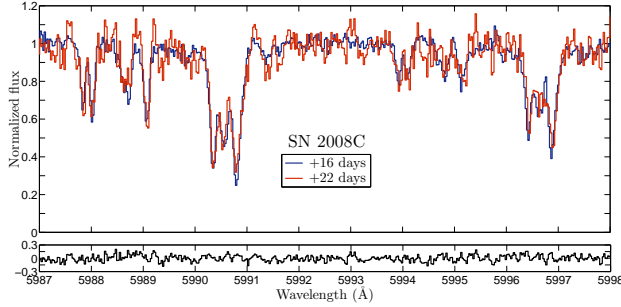


Figure 4. The dual-epoch spectra of SN 2008C. The first epoch is given in blue while the second is given in red. The difference spectrum (black line) is given in the narrow panel at the bottom of the plot.

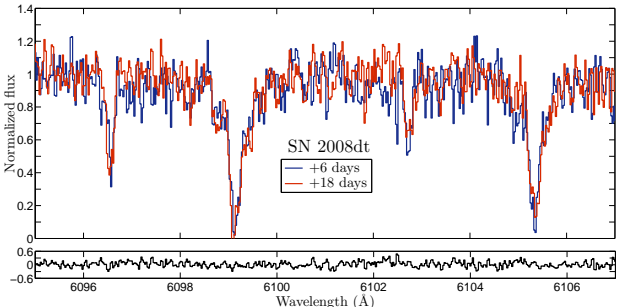
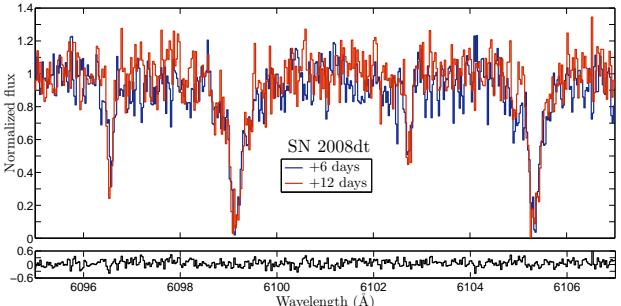


Figure 5. The triple-epoch spectra of SN 2008dt. Color code is the same as in previous figures. The upper panel shows the first and second epochs and the middle panel shows the first and third.

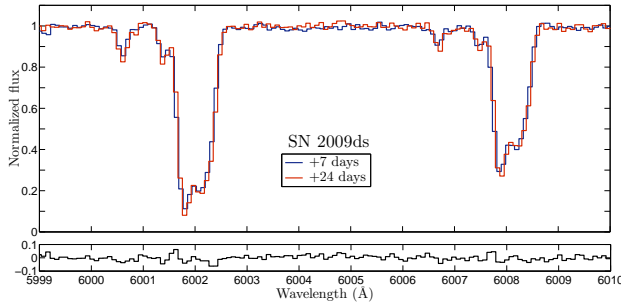


Figure 6. The dual-epoch spectra of SN 2009ds. Color code is the same as in the previous figures.

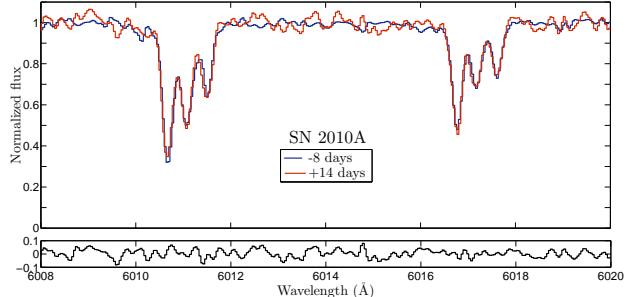
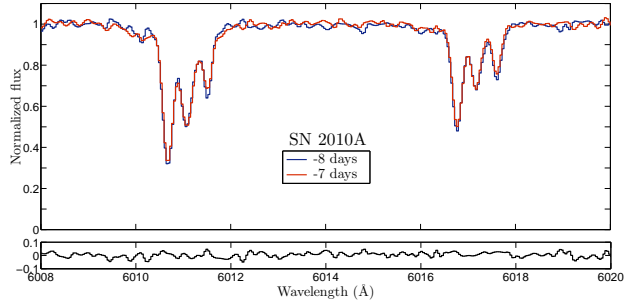


Figure 7. The triple-epoch spectra of SN 2010A.

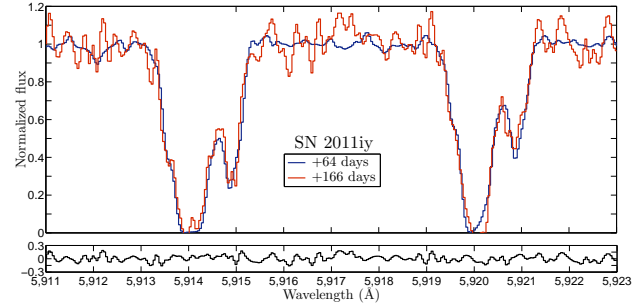


Figure 8. The dual-epoch spectra of SN 2011iy.

Table 2. Measurements for the previously published events.

	Phase (days since max)	EW (mÅ)		S/N
		D ₂	D ₁	
SN 2006X ¹	-2	828±3	688±3	78
	14	1137±2	882±2	101
	61	1206±4	947±4	56
	121	1147±12	918±12	20
SN 2007le ²	-5	894±3	649±3	113
	0	883±4	661±5	71
	10	906±20	695±20	16
	12	949±4	702±5	76
PTF 11kx ^{1,3}	84	1006±7	766±7	46
	-1	75±13	124±13	21
	9	172±12	91±12	24
	20	292±20	190±20	14
	44	199±19	183±19	15

¹ New measurements.

² Taken from Simon et al. (2009).

³ Measured only on the variable features.

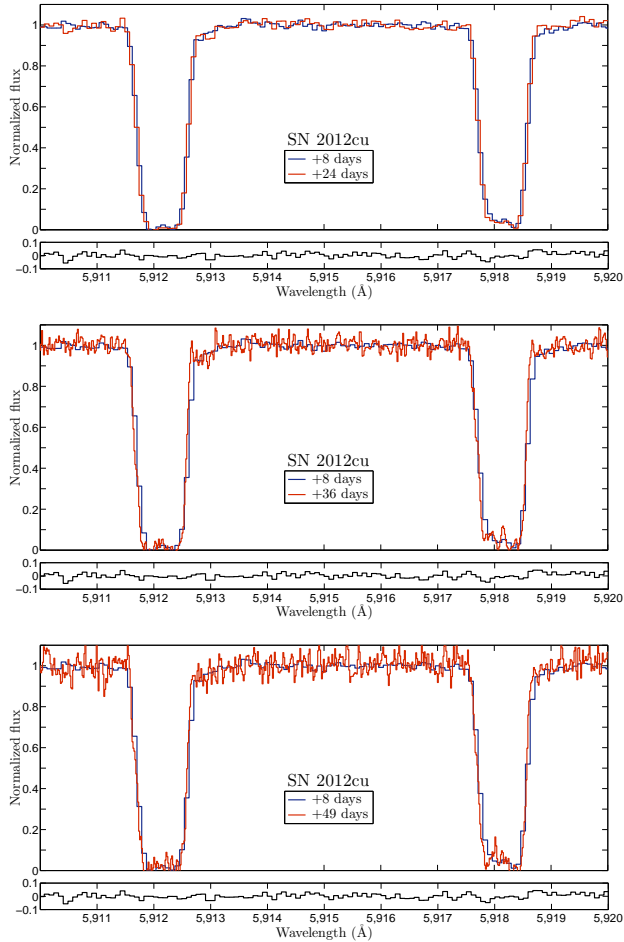


Figure 9. The multi-epoch spectra of SN 2012cu.

the stronger D_2 lines should have shown a greater disagreement, yet they do not.

The second epoch of SN 2011iy was obtained with very poor S/N. Even though some variability is seen in Fig. 8 the difference spectrum shows that the difference is well within the noise level. The variations in the absorption lines are of the same order as the variations seen in the continuum between the doublet. Moreover, the values of the EW are in agreement within 1.1σ .

All four epochs of SN 2012cu seem to be well in agreement with one another as seen in Fig. 9. The EW values also agree with each other quite well. The largest disagreement is a 2.3σ difference between the EW of the D_1 features measured for the first and third epochs. The lines are highly saturated.

There are some very weak features around 5919\AA in the spectra of SN 2012fr (see Fig. 10). These are slightly under-subtracted telluric features. Otherwise the region seems to be featureless on all epochs. SN 2012ht and SN 2013aa also exhibit featureless spectra, see Fig. 12 and 13 respectively.

The spectra of SN 2012hr are presented in Fig. 11. We can see that the comparison between the two epochs does not reveal significant variability. Though the red-most D_2 feature shows a slight decrease in intensity this is not observed in the D_1 feature. In addition, the EW values of the D_2 features are consistent within a 1.3σ level.

The two epochs of SN 2013aj are presented in Fig. 14. While

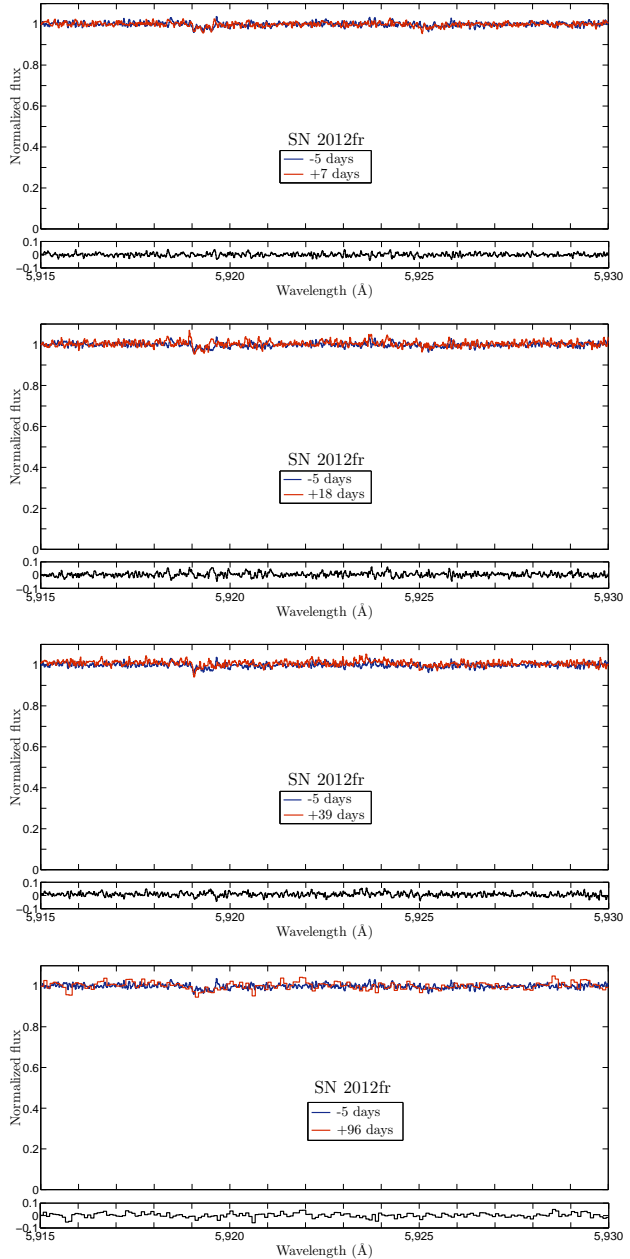


Figure 10. The multi-epoch spectra of SN 2012fr. SN or galaxy ($z = 0.005457$) Na I D features are expected to appear around 5922\AA & 5928\AA (D_2 and D_1 , respectively). The very weak features around 5919\AA are slightly under-subtracted telluric features. No host or SN features are observed.

the blue-most feature of the sodium doublet appears to experience some strengthening, the EWs of both epochs agree with each other within the 1σ level. Moreover, the difference spectrum shows that the differences are within the noise level.

To summarize, 13 of the SNe Ia presented in this study do not exhibit significant time-variable absorption features that could be indicative of the presence of CSM along the line-of-sight to these events. The difference spectra of these events are consistent with zero within the S/N. In contrast, an examination of SN 2006X, SN 2007le, and PTF 11kx, the three previously published events for which time-variability was detected in high-resolution-spectra,

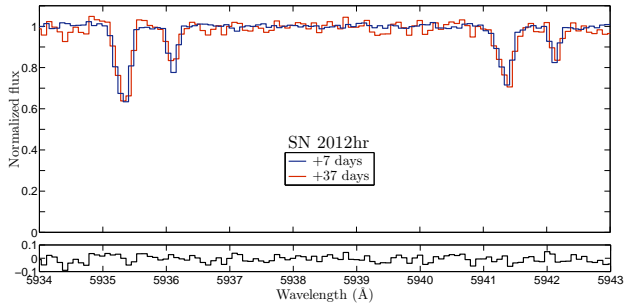


Figure 11. The dual-epoch spectra of SN 2012hr. The observed variability in the D_2 red-most feature ($\sim 5936.05\text{\AA}$) is both not observed in the corresponding D_1 line and within the calculated errors.

clearly reveals the time-variability in the Na I D absorption features. One SN, 2009ds, does indeed exhibit variability. This variability is not as profound as the variability exhibited in the previously published detections, and in the next section we will discuss whether this variability is indicative of CSM or whether it is consistent with other explanations.

4 DISCUSSION

Comparing the shape and EW of the sodium D line features exhibited in the SN Ia events presented in this study reveals no significant time-variability that may be associated with CSM in all but one case, SN 2009ds. A question immediately arises what is the cause of this variability. The measured change in EW is $\Delta EW_{D_2} = 28 \pm 8\text{m\AA}$ and $\Delta EW_{D_1} = 13 \pm 8\text{m\AA}$. This change is small compared to the variability observed in SN 2006X, SN 2007le, and PTF 11kx. It is comparable to the observed variability in SN 2011fe, $\Delta EW_{D_2} = 15.6 \pm 6.5\text{m\AA}$ (Patat et al. 2013), which was shown to be consistent with the expected short time-scale variations in interstellar absorptions produced by an expanding SN photosphere combined with a patchy ISM (Patat et al. 2010). Therefore, even if the observed variability is real we conclude that it is most likely associated to the ISM and not to the CSM environment of SN 2009ds.

As to whether the reported non-detections are robust. A robust non-detection should have an early first epoch that can serve as a good zero point with which to compare later epochs. As the CSM, if present, begins to recombine after maximum light, the initial epoch should be obtained around maximum light. An initial spectrum obtained later, might have been obtained after some, or all, of the CSM has recombined, and will not serve as a good zero point for comparison.

The first spectra of both SN 2007sa and SN 2011iy were obtained more than 60 days after maximum light. Based on previous CSM detections we expect that by this phase any CSM that was ionized by the UV flash will have already re-combined (see Fig. 15). Therefore, such late spectra cannot rule out variability at earlier stages and therefore should not be used as a non-detection and should not be included in statistical analysis of multi-epoch high-spectral-resolution samples of SNe Ia.

Based on previous cases (SN 2006X, SN 2007le, and PTF 11kx) we cannot determine that any variability would have been seen between the two closely-spaced epochs we have for SN 2008C (days +18 and +22; see Fig. 15). So, we argue that this non-detection should not be considered robust. This case empha-

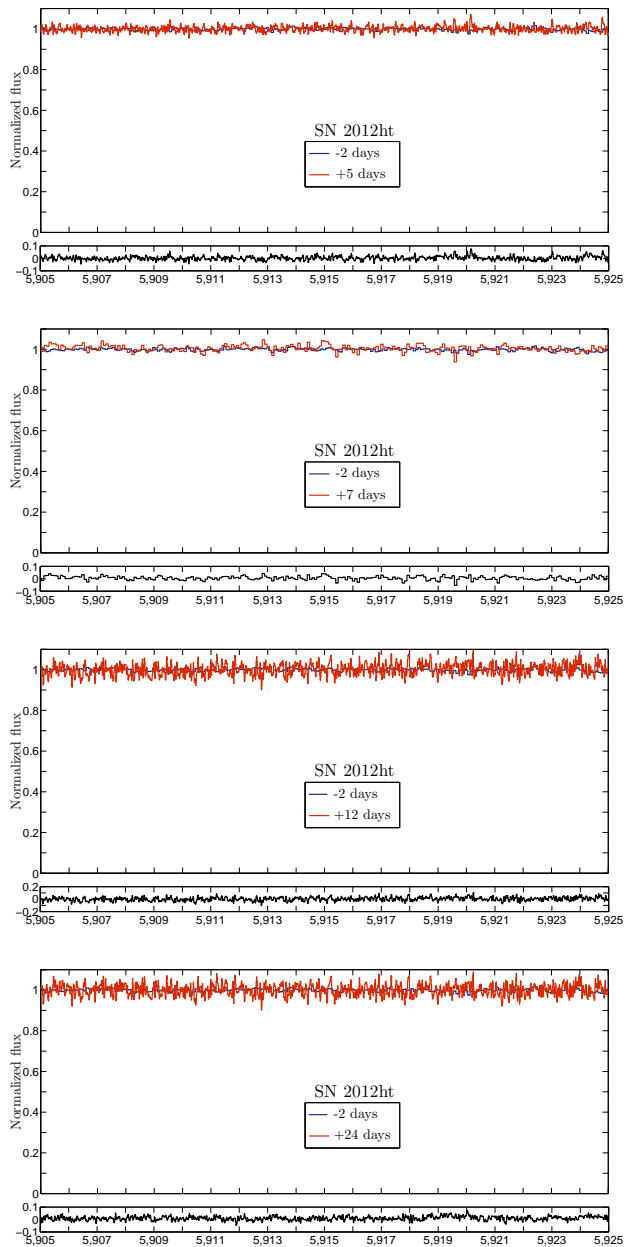


Figure 12. The multi-epoch spectra of SN 2012ht. SN or host galaxy ($z = 0.003559$) Na I D features are expected to appear around 5911\AA & 5917\AA . No features are observed.

sizes the need for an early-time first epoch and at least on more well spaced epoch.

The first epochs of the remaining 11 events were obtained no later than 8 days after maximum light. If we disregard epochs of SN 2006X, SN 2007le, and PTF 11kx that were obtained earlier than 8 days we can still observe significant time-variability in all three events. Therefore, we argue that the non-detection reported for these events are robust. This criterion will have to be revised if future observations will show events for which all the time-variability occurs earlier than 8 days after maximum light.

The D_1/D_2 ratio for many of our events is considerably larger than 0.5, the ratio for optically thin gas. In the optically thick regime the line profiles are less sensitive to changes in the column density, making them harder to identify, especially in low S/N

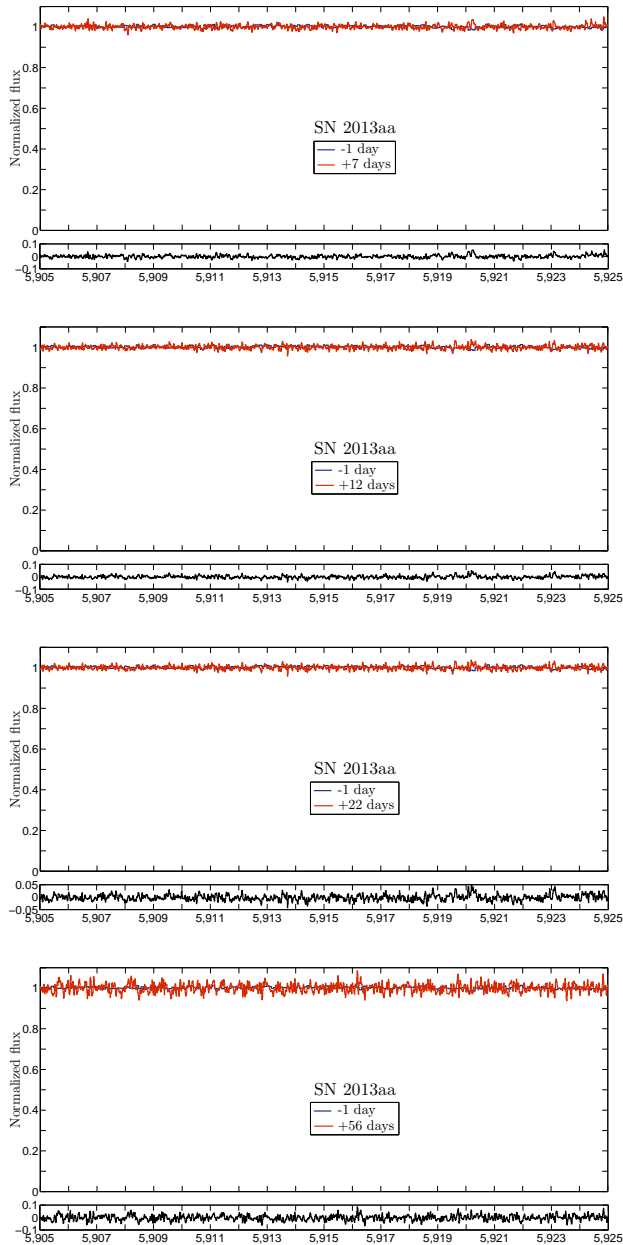


Figure 13. The multi-epoch spectra of SN 2013aa. SN or host galaxy ($z = 0.003999$) Na I D features are expected to appear around 5913.5Å & 5919.5Å. No features are observed.

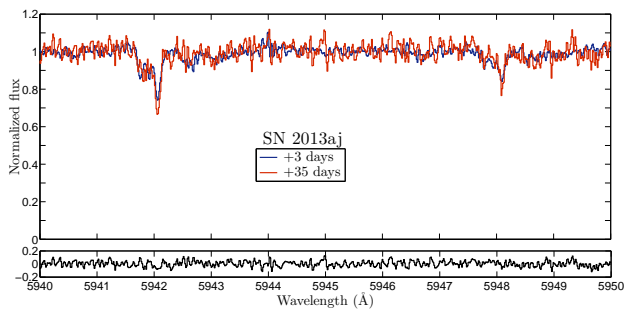


Figure 14. The dual-epoch spectra of SN 2013aj.

spectra. Nevertheless, the obvious fact that we do not observe time variability in the spectra of these events at these epochs is an indication that the environment along the line-of-sight to these events is different with respect to that along the line-of-sight to SN 2006X, SN 2007le, and PTF 11kx.

In addition, we cannot rule out the presence of weak absorption lines that will be undetectable due to the noise in the spectra. Following Leonard & Filippenko (2001), one can quantify the upper detection limit when no features are apparent in the spectrum as,

$$W_{\lambda}(3\sigma) = 3\Delta\lambda\Delta I \sqrt{\frac{W_{line}}{\Delta\lambda}} \sqrt{\frac{1}{B}}, \quad (1)$$

where $\Delta\lambda$ is the spectral resolution, ΔI the root-mean-square fluctuations of the normalized flux, W_{line} is the width of the feature, and B is the number of bins per resolution element. Assuming that these lines are optically thin we can follow (Spitzer 1978, §3.4.c) and use the curve-of-growth to convert equivalent width into column densities using,

$$N = \frac{m_e c^2}{\pi e^2} \frac{W_{\lambda}}{f\lambda^2} = 1.13 \times 10^{20} \frac{W_{\lambda}}{f\lambda^2}, \quad (2)$$

where f is the oscillator strength. Given the different spectral resolution of the different instruments and the S/N of the different observations, and assuming $W_{\lambda} = 0.2\text{Å}$, we can conclude that any feature arising from a Na I column density of more than a few times 10^{10} cm^{-2} should have been detectable in the spectra of the majority of these events. The extreme cases are SN 2012fr, for which the detectability limit is $\sim 7.8 \times 10^9 \text{ cm}^{-2}$ and SN 2007on and SN 2008dt, for which the limits are $6 \times 10^{10} \text{ cm}^{-2}$ and $8 \times 10^{10} \text{ cm}^{-2}$, respectively. Therefore, a line-of-sight environment similar to those observed for SN 2006X, SN2007le, and PTF 11kx should have produced detectable lines. Assuming all the sodium is neutral and a solar abundance ratio, $\log Na/H = -6.3$, we get a hydrogen column density limit of $\sim 10^{17} \text{ cm}^{-2}$. Assuming this material is distributed in a thin spherical shell at radius R the mass of the shell will be,

$$M_{shell} \simeq \left(\frac{R}{10^{17} \text{cm}} \right)^2 \times 10^{-5} M_{\odot}, \quad (3)$$

though this estimate is only a rough estimate and most likely an over estimate. For SN 2012fr the limit is approximately one order of magnitude lower.

Our spectroscopic observations only probe the CSM along the line-of-sight, therefore, we cannot rule out presence of material off the line-of-sight. Nevertheless, simulations of proposed progenitor systems (e.g., Mohamed, Booth & Podsiadlowski 2013; Shen, Guillochon & Foley 2013; Raskin & Kasen 2013) may offer an insight to whether they can form CSM in a way that allows for line-of-sight environments that are consistent with our observations, especially the relatively clean featureless line-of-sights observed toward SN 2007on, SN 2012fr, SN 2012ht, and SN 2013aa. Such a comparison between theoretical results and the observed multi-epoch high-spectral-resolution sample can be highly insightful, but remains beyond the scope of this paper.

5 CONCLUSIONS

Our data extends the published multi-epoch high-spectral-resolution sample size to 17 events for which robust detection or non-detection can be claimed. Three events exhibit time-variable

Na I D features attributed to CSM. Assuming Poisson statistics we find that $18\% \pm 11\%$ ($19\% \pm 12\%$ if we exclude SN 2007on which occurred in an elliptical host) of the events in the enlarged sample exhibit time-variable features that can be associated with CSM. This result is in agreement with the results of S11 and Maguire et al. (2013) who estimated the fraction to be 20 – 25% of nearby SNe Ia in late-type galaxy hosts. This estimate is a lower limit as CSM may lay off the line-of-sight or on the line-of-sight but further away from the progenitor system. In the first case this material will not be visible in the spectrum. In the later, the CSM lines will not vary with time and be regarded as a non-detection. Moreover, though this is the largest multi-epoch high-spectral-resolution SN Ia sample to date it is still relatively small. A larger sample will be useful to shed light on the ratio between SNe Ia with CSM and those without. This ratio and the study of the properties of detected CSM can help us to disentangle the different proposed channels leading to SNe Ia explosions. In order for the published multi-epoch high-spectral-resolution sample to be more complete and not biased toward events with detected time-variability it is critical to publish all the observed events. With the publication of this data set the sample of SNe Ia observed by the Keck-Magellan effort till 2009 is complete. The VLT 2008–2009 sample is still being worked on and will be soon published (Cox et al., in preparation).

ACKNOWLEDGMENTS

A.S. is supported by a Minerva Fellowship. The research of A.G. is supported by the EU/FP7 via an ERC grant no. 307260, the Minerva ARCHES prize and the Kimmel award.

The authors would like to acknowledge the generosity of the late Wallace L. W. Sargent in providing data. The authors would also like to acknowledge the help of D. J. Osip and J. F. Steiner in obtaining the data.

Partially based on observations made with ESO Telescopes at the La Silla Paranal Observatory, Chile, under programme ID 289.D-5023, 290.D-5010, 290.D-5023, 091.D-0780.

This paper includes data gathered with the 6.5 meter Magellan Telescopes located at Las Campanas Observatory, Chile.

Some of the data presented herein were obtained at the W.M. Keck Observatory, which is operated as a scientific partnership among the California Institute of Technology, the University of California and the National Aeronautics and Space Administration. The Observatory was made possible by the generous financial support of the W.M. Keck Foundation. The authors wish to recognize and acknowledge the very significant cultural role and reverence that the summit of Mauna Kea has always had within the indigenous Hawaiian community. We are most fortunate to have the opportunity to conduct observations from this mountain.

REFERENCES

- Agnoletto I., Harutyunyan A., Benetti S., Turatto M., Cappellaro E., Deneffeld M., Adami C., 2007, Central Bureau Electronic Telegrams, 1163, 1
- Anderson J., Morrell N., Folatelli G., Stritzinger M., 2009, Central Bureau Electronic Telegrams, 1789, 1
- Ayani K., Yamaoka H., 2008, Central Bureau Electronic Telegrams, 1197, 1
- Bernstein R., Sheckman S. A., Gunnels S. M., Mochnacki S., Athey A. E., 2003, in Society of Photo-Optical Instrumentation Engineers (SPIE) Conference Series, Vol. 4841, Society of Photo-Optical Instrumentation Engineers (SPIE) Conference Series, Iye M., Moorwood A. F. M., eds., pp. 1694–1704
- Blondin S., Berlind P., 2008, Central Bureau Electronic Telegrams, 1424, 1
- Blondin S., Prieto J. L., Patat F., Challis P., Hicken M., Kirshner R. P., Matheson T., Modjaz M., 2009, ApJ, 693, 207
- Brimacombe J. et al., 2013, Central Bureau Electronic Telegrams, 3434, 1
- Challis P., Calkins M., 2009, Central Bureau Electronic Telegrams, 1788, 2
- Childress M., Zhou G., Tucker B., Bayliss D., Scalzo R., Yuan F., Schmidt B., 2012, Central Bureau Electronic Telegrams, 3275, 2
- Clough S. A., Shephard M. W., Mlawer E. J., Delamere J. S., Iacono M. J., Cady-Pereira K., Boukabara S., Brown P. D., 2005, J. Quant. Spectrosc. Radiat. Transfer, 91, 233
- Cox L., Newton J., Puckett T., Orff T., 2010, Central Bureau Electronic Telegrams, 2109, 1
- Dekker H., D’Odorico S., Kaufer A., Delabre B., Kotzłowski H., 2000, in Society of Photo-Optical Instrumentation Engineers (SPIE) Conference Series, Vol. 4008, Society of Photo-Optical Instrumentation Engineers (SPIE) Conference Series, Iye M., Moorwood A. F., eds., pp. 534–545
- Dilday B. et al., 2012, Science, 337, 942
- Drake A. J., Djorgovski S. G., Williams R., Mahabal A., Graham M. J., Christensen E., Beshore E. C., Larson S. M., 2007, The Astronomer’s Telegram, 1337, 1
- Drescher C. et al., 2012, Central Bureau Electronic Telegrams, 3346, 1
- Foley R. J., Esquerdo G., 2010, Central Bureau Electronic Telegrams, 2112, 1
- Foley R. J. et al., 2012, ApJ, 752, 101
- Gal-Yam A., Simon J., Klotz A., Rosolowsky E., 2007, The Astronomer’s Telegram, 1263, 1
- Graham A. W., Colless M. M., Busarello G., Zaggia S., Longo G., 1998, A&AS, 133, 325
- Hoyle F., Fowler W. A., 1960, ApJ, 132, 565
- Iben, Jr. I., Tutukov A. V., 1984, ApJS, 54, 335
- Ilkov M., Soker N., 2012, MNRAS, 419, 1695
- Itagaki K., Brimacombe J., Noguchi T., Nakano S., 2011, Central Bureau Electronic Telegrams, 2943, 1
- Itagaki K. et al., 2012, Central Bureau Electronic Telegrams, 3146, 1
- Kashi A., Soker N., 2011, MNRAS, 417, 1466
- Klotz A. et al., 2012, Central Bureau Electronic Telegrams, 3275, 1
- Leonard D. C., Filippenko A. V., 2001, PASP, 113, 920
- Libbrecht K. G., Peri M. L., 1995, PASP, 107, 62
- Livio M., Riess A. G., 2003, ApJ, 594, L93
- Madison D., Li W., Filippenko A. V., 2008, Central Bureau Electronic Telegrams, 1423, 1
- Maguire K. et al., 2013, accepted for publication in MNRAS
- Mannucci F., Della Valle M., Panagia N., 2006, MNRAS, 370, 773
- Marion G. H., Milisavljevic D., Rines K., Wilhelmy S., 2012, Central Bureau Electronic Telegrams, 3146, 2
- Mazzali P. A., 2000, A&A, 363, 705
- Mohamed S., Booth R., Podsiadłowski P., 2013, in Astronomical Society of the Pacific Conference Series, Vol. 469, 18th European White Dwarf Workshop., Krzesiń, ski J., Stachowski G., Moskalik P., Bajan K., eds., p. 323
- Morrell N., Phillips M. M., Contreras C., Roth M., Hsiao E. Y., Marion G. H., Stritzinger M., 2012, The Astronomer’s Telegram, 4663, 1
- Mostardi R., Li W., 2007, Central Bureau Electronic Telegrams, 1161, 1
- Naito H., Sakane Y., Anan T., Kouzuma S., Yamaoka H., 2007, Central Bureau Electronic Telegrams, 1173, 1
- Nakano S., Itagaki K., Kadota K., Wells W., Nissinen M., Hentunen V.-P., 2009, Central Bureau Electronic Telegrams, 1784, 1
- Parker S., Amorim A., Parrent J. T., Sand D., Valenti S., Graham M. L., Howell D. A., 2013, Central Bureau Electronic Telegrams, 3416, 1
- Parrent J. T., Sand D., Valenti S., Graham M. J., Howell D. A., 2013, The Astronomer’s Telegram, 4817, 1
- Patat F. et al., 2007a, A&A, 474, 931
- Patat F. et al., 2007b, Science, 317, 924
- Patat F. et al., 2013, A&A, 549, A62

Patut F., Cox N. L. J., Parrent J., Branch D., 2010, *A&A*, 514, A78
 Pauldrach A. W. A., Duschinger M., Mazzali P. A., Puls J., Lennon M., Miller D. L., 1996, *A&A*, 312, 525
 Pojmanski G., Prieto J. L., Stanek K. Z., Beacom J. F., 2008, Central Bureau Electronic Telegrams, 1213, 1
 Pollas C., Klotz A., 2007, Central Bureau Electronic Telegrams, 1121, 1
 Puckett T., Gagliano R., Newton J., Orff T., 2008, Central Bureau Electronic Telegrams, 1195, 1
 Raskin C., Kasen D., 2013, *ApJ*, 772, 1
 Rothman L. S. et al., 2009, *J. Quant. Spectrosc. Radiat. Transfer*, 110, 533
 Shen K. J., Guillochon J., Foley R. J., 2013, *ApJ*, 770, L35
 Simon J. D. et al., 2009, *ApJ*, 702, 1157
 Simon J. D. et al., 2007, *ApJ*, 671, L25
 Sparks W. M., Stecher T. P., 1974, *ApJ*, 188, 149
 Spitzer L., 1978, *Physical processes in the interstellar medium*
 Sternberg A. et al., 2011, *Science*, 333, 856
 Stritzinger M. D. et al., 2011, *AJ*, 142, 156
 Sullivan M. et al., 2010, *MNRAS*, 406, 782
 Vogt S. S. et al., 1994, in *Society of Photo-Optical Instrumentation Engineers (SPIE) Conference Series*, Vol. 2198, Society of Photo-Optical Instrumentation Engineers (SPIE) Conference Series, Crawford D. L., Craine E. R., eds., p. 362
 Wang X., Wang L., Filippenko A. V., Zhang T., Zhao X., 2013, *Science*, 340, 170
 Webbink R. F., 1984, *ApJ*, 277, 355
 Whelan J., Iben, Jr. I., 1973, *ApJ*, 186, 1007
 Yamanaka M., Ui T., Arai A., 2011, Central Bureau Electronic Telegrams, 2943, 3
 Yusa T. et al., 2012, Central Bureau Electronic Telegrams, 3349, 1
 Zhang T.-M., Lin M.-Y., Wang X.-F., 2012, Central Bureau Electronic Telegrams, 3146, 3

APPENDIX A: DESCRIPTION OF THE OBSERVATIONS

In this appendix we provide information regarding the discovery and spectroscopic observations of each SN in the presented sample.

SN 2007on was discovered on 2007-11-05.25 UT (all dates in this paper are given in UT) 12" west and 68" north of the center of the elliptical galaxy NGC 1404 (Pollas & Klotz 2007) and reported to be a young SN Ia on 2007-11-06 (Gal-Yam et al. 2007). Based on the Carnegie Supernova Project photometric data¹ SN 2007on maximum light in B band occurred around 2007-11-16. HIRES spectra of SN 2007sa were obtained on 2007-11-20.3 and 2008-01-16.2. The first observation was performed 4 days after B band maximum light.

SN 2007sa was discovered on 2007-11-21.56 1".8 west and 7".7 north of the nucleus of NGC 3499 (Mostardi & Li 2007) and reported to be a SN Ia one month after maximum light on 2007-12-12.14 (Agnolletto et al. 2007). HIRES observations of SN 2007sa were performed on 2008-01-17.4 and 2008-01-23.59. Both spectroscopic epochs were obtained quite late (the first one 66 days after maximum light) and fairly close together, reducing the sensitivity to variable absorption.

SN 2007sr was discovered on 2007-12-18.53 on the southern arm of the antennae galaxies emanating from NGC 4038 (Drake et al. 2007), at 4 days after maximum light (Pojmanski et al. 2008). SN 2007sr was classified as a SN Ia on 2007-12-19 (Naito et al. 2007). SN 2007sr was observed using MIKE on 2007-12-20, 2007-12-21, and 2007-12-22, using EAE on 2007-12-24, and using HIRES on 2008-01-17. The first epoch was obtained around 6 days after maximum light.

SN 2008C was discovered on 2008-01-03.27 2".95 west of the center of UGC 3611 (Puckett et al. 2008) and confirmed as a SN Ia near maximum

light on 2008-01-04.8 (Ayani & Yamaoka 2008). SN 2008C was observed using HIRES on 2008-01-17.64 and 2008-01-23.55. SN 2008C was spectrally typed as a normal Type Ia (Stritzinger et al. 2011). The first epoch observation was performed 16 days after maximum light (Foley et al. 2012).

SN 2008dt was discovered on 2008-06-30.33 1".0 east and 5".5 south of the nucleus of NGC 6261 (Madison, Li & Filippenko 2008) and confirmed as a SN Ia around one week before maximum light on 2008-07-01.21 (Blondin & Berlind 2008). SN 2008dt was observed using HIRES on 2008-07-06.48, 2008-07-12.48 and 2008-07-18.46. The first epoch observation was performed 6 days after maximum light (Foley et al. 2012).

SN2009ds was discovered on 2009-04-28.56 12" west and 3" north of the center of NGC 3905 (Nakano et al. 2009) and confirmed as a normal SN Ia around one week before maximum light on 2009-04-29.6 (Challis & Calkins 2009; Anderson et al. 2009). MIKE observations of SN 2009ds were performed on 2009-05-15.96 and 2009-06-01.97. The first epoch observation was performed around 7 days after maximum light.

SN 2010A was discovered on 2010-01-04.14 2".4 east and 6".9 north of the center of UGC 2019 (Cox et al. 2010), and classified as a normal Type Ia at 9 days before maximum brightness on 2010-01-07 (Foley & Esquerdo 2010). SN 2010A was observed with MIKE on 2010-01-08, 2010-01-09, and 2010-01-30. The first epoch spectrum was obtained about 8 days before maximum light.

SN 2011iy was discovered on 2011-12-09.86 16".6 east and 6".1 south of the center of NGC 4984 (Itagaki et al. 2011), and classified as a Type Ia at 12 days after maximum light on 2011-12-14.81 (Yamanaka, Ui & Arai 2011). SN 2011iy was observed with MIKE on 2012-02-04.26 and 2012-06-06.12. The first epoch spectrum was obtained about 64 days after maximum light.

SN 2012cu was discovered on 2012-06-11.1 3".1 east and 27".1 south of the nucleus of NGC 4772 (Itagaki et al. 2012), and was classified as a SN Ia 7 days before maximum light (Marion et al. 2012; Zhang, Lin & Wang 2012). MIKE observations were performed on 2012-06-30.01 and 2012-07-16.03. UVES observations were performed on 2012-07-28.99 and 2012-08-10.98. The first epoch observation was performed around 8 days after maximum light.

SN 2012fr was discovered on 2012-10-27.05 3" west and 52" north of the nucleus of NGC 1365 (Klotz et al. 2012), and classified as a Type Ia on 2012-10-28.53 (Childress et al. 2012). Observations with UVES were performed on 2012-11-07.16, 2012-11-19.08, 2012-12-02.13, and 2012-12-21.05, and with MIKE on 2013-02-16.01. The first epoch spectrum was obtained around about 5 days before maximum light.

SN 2012hr was discovered on 2012-12-16.533 2".3 west and 93".6 north of the center of ESO 121-26 (Drescher et al. 2012). SN 2012hr was classified as a SN Ia approximately 1 week before maximum light on 2012-12-20.2 (Morrell et al. 2012). MIKE observations were performed on 2013-01-02 and 2013-02-01. The first epoch spectrum was obtained about 7 days after maximum light.

SN 2012ht was discovered on 2012-12-18.77 19" west and 16" north of the center of NGC 3447 and classified as a SN Ia 7 days before maximum light on 2012-12-20.4 (Yusa et al. 2012). Based on Swift lightcurves maximum light occurred around 2013-01-04². Observations with MIKE were performed on 2013-01-02.29 and 2013-01-11.33, and with UVES on 2013-01-09.34, 2013-01-16.34, and 2013-01-28.28. The first epoch observation was performed around 2 days before maximum light.

2013aa was discovered 2013-02-13.62 74" west and 180" south of the center of NGC 5643 (Parker et al. 2013). SN 2013aa was classified as a

¹ <http://csp.obs.carnegiescience.edu/data/lowzSNe/SN2007on/>

² http://people.physics.tamu.edu/pbrown/SwiftSN/SN2012ht_lightcurve.jpg

Type Ia a few days before maximum light on 2013-02-15.38 (Parrent et al. 2013). SN2013aa was observed with MIKE on 2013-02-16.38 and with UVES on 2013-02-24.31, 2013-03-01.31, 2013-03-11.39, and 2013-04-14.3. The first epoch spectrum was obtained about 1 days before maximum light.

2013aj was discovered on 2013-03-03.14 5".7 east and 8" north of the center of NGC 5339 and was classified on the same night as a SN Ia 7 days before maximum light (Brimacombe et al. 2013). Observations with UVES were performed on 2013-03-13.29 and 2013-04-14.24. The first epoch observation was performed around 3 days after maximum light.